

Proline-Based Block Copolymers Displaying Upper and Lower Critical Solution Temperatures

Hideharu Mori,^{*,†} Ikumi Kato,[†] Shoko Saito,[†] and Takeshi Endo[‡]

[†]Department of Polymer Science and Engineering, Graduate School of Science and Engineering, Yamagata University, 4-3-16, Jonan, Yonezawa 992-8510, Japan and [‡]Molecular Engineering Institute, Kinki University, Iizuka, Fukuoka 820-8555, Japan

Received September 7, 2009; Revised Manuscript Received December 15, 2009

ABSTRACT: Novel dual thermoresponsive block copolymers displaying lower critical solution temperature (LCST) and upper critical solution temperature (UCST) were synthesized by reversible addition–fragmentation chain transfer (RAFT) polymerization of two proline-based monomers. Poly(*N*-acryloyl-L-proline methyl ester), poly(A-Pro-OMe), was selected as a thermoresponsive segment, whereas poly(*N*-acryloyl-4-*trans*-hydroxy-L-proline), poly(A-Hyp-OH), could be regarded as a water-soluble polymer. The block copolymer having suitable comonomer composition (A-Pro-OMe/A-Hyp-OH = 27/73) exhibited soluble–insoluble–soluble transition with lower (LCST = 19–21 °C) and upper (UCST = 39–45 °C) critical solution temperatures in acidic water. The comonomer composition of poly(A-Pro-OMe)-*b*-poly(A-Hyp-OH) and pH value in the aqueous solution were found to affect characteristic thermoresponsive behaviors. The temperature-dependent assembled structures and chiroptical properties were evaluated by dynamic light scattering (DLS) and circular dichroism (CD) measurements. Another type of dual thermosensitive block copolymers with blocks having two different LCSTs, poly(A-Pro-OMe)-*b*-poly(A-Hyp-OMe), were prepared by the methylation of the carboxylic acid groups in poly(A-Pro-OMe)-*b*-poly(A-Hyp-OH), and their temperature-dependent solution behaviors were investigated. To the best of our knowledge, this is the first report of the dual thermoresponsive system, which can be changed from a system exhibiting LCST and UCST into another one having two different LCSTs by a simple methylation reaction.

Introduction

Stimuli-responsive materials, so-called “intelligent” or “smart” materials, have been extensively studied from both scientific and technological points of view.^{1–8} Thermosensitive block copolymers are an important research central to developments in this fields because temperature-induced self-assemble behaviors, such as normal and reversible micelle formation, are observed above a critical point (lower critical solution temperature, LCST) or below a certain temperature (upper critical solution temperature, UCST).^{7–11} Recently, double- or multi-stimuli-sensitive copolymers and gels that can sense two or more signals and produce a definite dynamic response in the form of a change in shape, size, or structure have attracted significant research interest.^{7,8,12–14} In addition to property of each segment, composition, and chain length of the block copolymers, assembled structures of the stimuli-responsive block copolymers can be govern by external stimuli such as pH, salt, and temperature. A number of thermoresponsive block copolymers, which are also sensitive to another stimulus, have been developed so far.^{11,13,15–21}

Dual thermosensitive block copolymers can be classified into two categories: block copolymers with blocks displaying different LCSTs and block copolymers displaying LCST and UCST. As to the block copolymers consisting of two or more different thermosensitive moieties, a variety of systems have been reported, including block copolymers composed of *N*-isopropylacrylamide/*N*-acryloylpyrrolidine,²² vinyl ethers with pendant oxyethylene groups,²³ propylene oxide/ethoxyethyl glycidyl ether,²⁴ acrylate/styrene derivatives with pendant oxyethylene groups,²⁵

and *N*-isopropylacrylamide/propylene oxide.²⁶ These block copolymers consisting of two or more different thermosensitive moieties exhibited intriguing temperature-induced self-assembly behavior in water.

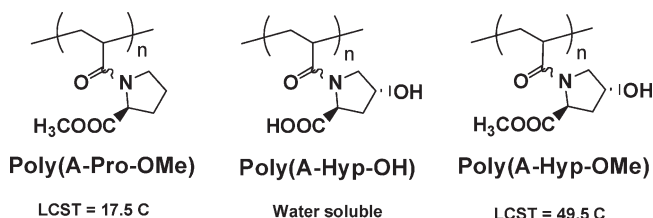
Compared with polymers having LCSTs in aqueous media, polymers exhibiting UCST-type insoluble–soluble transition are relatively uncommon. Poly(sulfobetaine)²⁷ and poly(acrylic acid)²⁸ are reported to exhibit UCST, and these polymers commonly have a pair of interactive sites that cause the polymer to be insoluble at low temperatures due to intra- and interchain interactions such as hydrogen bonding and electrostatic attractions. Laschewsky reported that the schizophrenic block copolymers prepared from a nonionic monomer, *N*-isopropylacrylamide, and a zwitterionic monomer, 3-[*N*-(3-methacrylamidopropyl)-*N,N*-dimethyl]ammoniopropanesulfonate, exhibited LCST and UCST.^{10,29} Block copolymer displaying both LCST and UCST was also prepared by selective quaternization of poly(2-(dimethylamino)ethyl methacrylate)-*b*-poly(2-(*N*-morpholino)ethyl methacrylate) using 1,3-propane sultone.³⁰ Another example involve a diblock copolymer consisting of poly(3-dimethyl-(methacryloyloxyethyl)ammonium propanesulfonate) as an UCST block and poly(*N,N*-diethylacrylamide) as an LCST block.³¹ These block copolymers exhibited a core–corona inversion (micelle–unimer–inverse micelle transformation) simply depending on temperature. In contrast to these copolymers having zwitterionic segments, Baski reported that random copolymers comprising of acrylic acid with *N*-isopropylacrylamide presented both UCST and LCST.³² They demonstrated that chain shrinkage in the system is attributed to the formation of intrachain hydrogen bonds between the two complementary groups, acrylic acid and *N*-isopropylacrylamide, and the hydrophobicity of these

*To whom correspondence should be addressed; e-mail h.mori@yz.yamagata-u.ac.jp, Ph +81-238-26-3765, Fax +81-238-26-3749.

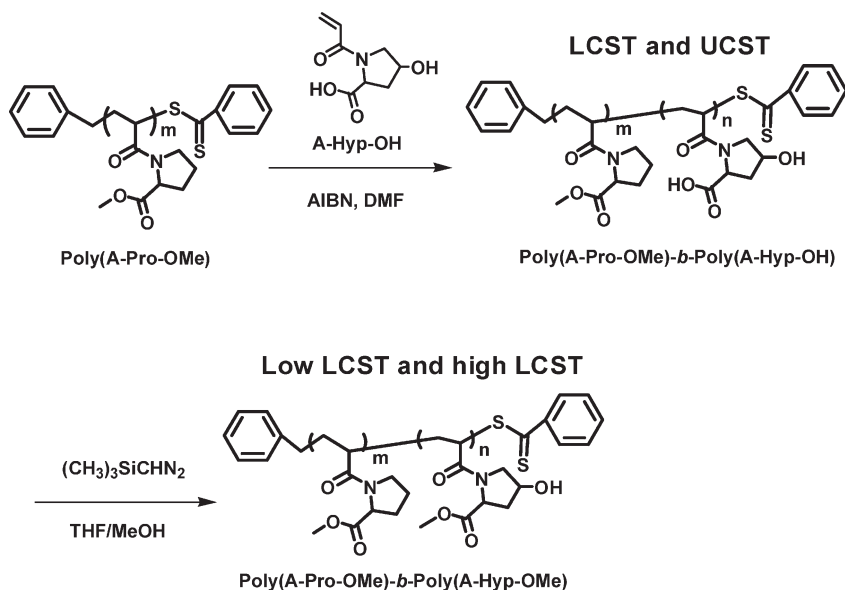
copolymers is strongly enhanced by intrachain hydrogen bonding. Similarly, several poly(*N*-vinylacetamide-*co*-acrylic acid)s containing more than 50% of *N*-vinylacetamide showed reentrant soluble–insoluble–soluble transitions with increasing temperature.³³ They demonstrated that introducing a hydrogen bonding pair and a polymer with moderate hydrophobicity afford a universal design for polymers with a soluble–insoluble–soluble transition in aqueous solution.

In this paper, we report the controlled synthesis of novel proline-based block copolymers that exhibit both LCST and UCST in aqueous media (Schemes 1 and 2). Reversible addition–fragmentation chain transfer (RAFT) polymerizations^{34–47} of two proline-based monomers, *N*-acryloyl-L-proline methyl ester (A-Pro-OMe) and *N*-acryloyl-4-*trans*-hydroxy-L-proline (A-Hyp-OH), were employed for the purpose. As a thermoresponsive segment, we selected poly(A-Pro-OMe), which processes a characteristic LCST-type soluble–insoluble transition at around 18 °C in a neutral water (pH = 7).^{45,46,48} Recently, we reported the synthesis of similar proline-based block copolymers displaying pH- and LCST-type thermoresponsive properties, which are comprised of A-Pro-OMe and *N*-acryloyl-L-proline having a carboxylic acid moiety in the monomer unit.⁴⁹ In this study, poly(A-Hyp-OH) was selected as a strong hydrophilic polymer as well as a weak polyelectrolyte, in which the degree of ionization of poly(A-Hyp-OH) is governed by the pH and ionic strength of aqueous solution. Since A-Hyp-OH has a carboxylic acid and a hydroxyl group in the monomer unit, poly(A-Hyp-OH) can also show specific interactions, such as hydrogen bonding, acid–base interactions, and oppositely charged ionic interactions, which may help to produce characteristic thermoresponsive properties.

Scheme 1. Structures of Thermoresponsive and Water-Soluble Polymers Used in This Study



Scheme 2. Synthesis of Block Copolymers by Reversible Addition–Fragmentation Chain Transfer (RAFT) Polymerization of *N*-Acryloyl-4-*trans*-hydroxy-L-proline (A-Hyp-OH) Using Poly(*N*-acryloyl-L-proline methyl ester), Poly(A-Pro-OMe), As a Macro-Chain Transfer Agent, Followed by Methylation



In this contribution, we mainly focused on proline-based block copolymers composed of poly(A-Pro-OMe) and poly(A-Hyp-OH), which exhibited soluble–insoluble–soluble transition with lower and upper critical solution temperatures in acidic water. The dual thermoresponsive behavior is due to the cooperative effect of the self-assembly of the block copolymer and hydrogen bonding between A-Pro-OMe and A-Hyp-OH units. In addition to the characteristic chiroptical properties, the dual thermoresponsive system of the proline-based block copolymer is different from previously reported ones; schizophrenic block copolymers showing micelle–unimer–inverse micelle transformation via self-assembly^{10,29,30} and random copolymers showing soluble–insoluble–soluble transition due to the formation/breaking of hydrogen bonding.^{32,33} Another advantage of the present system is the capability to change dual thermoresponsive properties from a system exhibiting LCST and UCST into another one having two different LCSTs by simple methylation reaction. The methylation reaction of the carboxylic acid groups in poly(A-Hyp-OH) led to thermoresponsive polymer, poly(A-Hyp-OMe), having a relatively higher phase separation temperature (49.5 °C).⁵⁰ In this study, we synthesized thermosensitive block copolymers with blocks having two different LCSTs, poly(A-Pro-OMe)-*b*-poly(A-Hyp-OMe), by the methylation of poly(A-Pro-OMe)-*b*-poly(A-Hyp-OH), as shown in Scheme 2.

Experimental Section

Materials. 2,2'-Azobis(isobutyronitrile) (AIBN, Kanto Chemical, 97%) was purified by recrystallization from ethanol. *N*-Acryloyl-L-proline methyl ester (A-Pro-OMe)⁵¹ and *N*-acryloyl-4-*trans*-hydroxy-L-proline (A-Hyp-OH)⁵⁰ were prepared by the reaction of acryloyl chloride with corresponding proline derivatives (L-proline methyl ester hydrochloride and 4-*trans*-hydroxy-L-proline, respectively) in accordance with the methods reported previously. The synthesis of benzyl dithiobenzoate was conducted according to the procedure reported previously.^{45,52} The chain transfer agent (CTA) was purified by vacuum distillation using a glass tube oven (Shibata GTO-250RS) to give a red oil. *N,N*-Dimethylformamide (dehydrated DMF, Kanto Chemical, 99.5%) was used as received. Chlorobenzene (Tokyo Kasei Kogyo, >98%) was dried with P₂O₅ and then distilled under vacuum. The methylation agent, trimethylsilyldiazomethane (2 M solution in diethyl ether), was purchased

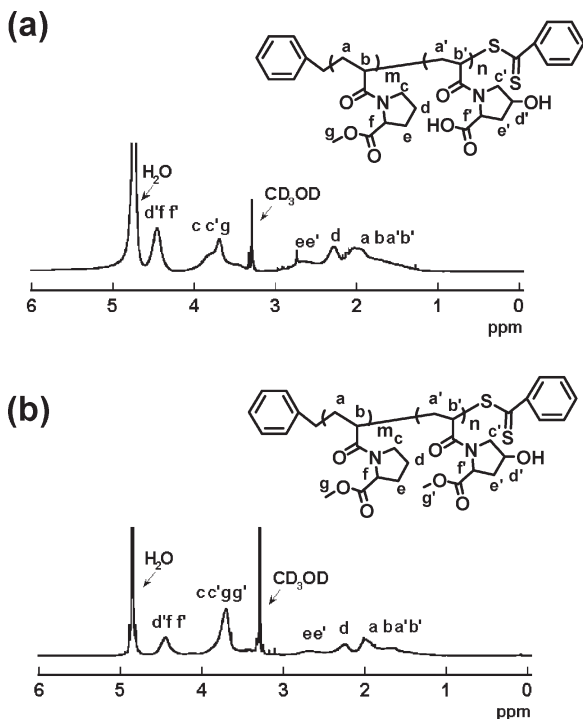


Figure 1. ^1H NMR spectra of (a) poly(A-Pro-OMe)-*b*-poly(A-Hyp-OH) and (b) poly(A-Pro-OMe)-*b*-poly(A-Hyp-OMe) in CD_3OD .

from Aldrich and used as received. All the other materials were used without further purification.

Synthesis of Block Copolymers. All polymerizations were performed in a degassed sealed tube with AIBN as the initiator. A representative example of the synthesis of the block copolymer comprising of A-Pro-OMe and A-Hyp-OH is as follows: A-Pro-OMe (1.00 g, 5.45 mmol), benzyl dithiobenzoate (26.6 mg, 0.11 mmol), AIBN (8.9 mg, 0.05 mmol), and chlorobenzene (4.0 mL) were placed in a dry ampule, and the solution was then degassed using three freeze–evacuate–thaw cycles. After the ampule was flame-sealed under vacuum, it was stirred at $60\text{ }^\circ\text{C}$ for 24 h. The reaction was stopped by rapid cooling with liquid nitrogen, and the monomer conversion (95%) was determined by the ^1H NMR spectrum of the polymerization mixture. The product was purified by precipitation into diethyl ether and then isolated by filtration. Finally, the resulting poly(A-Pro-OMe) was dried under vacuum at room temperature (yield = 99%, 0.99 g), which was used as a macro-CTA ($M_{n,\text{NMR}} = 6600$, $M_{n,\text{GPC}} = 6600$, $M_w/M_n = 1.27$).

The dithiobenzoate-terminated poly(A-Pro-OMe) (0.121 g, 0.018 mmol), AIBN (1.5 mg, 0.009 mmol), A-Hyp-OH (0.169 g, 0.91 mmol), and DMF (0.68 mL) were placed in a dry ampule. After the solution was degassed by three freeze–evacuate–thaw cycles, the polymerization was conducted at $60\text{ }^\circ\text{C}$ for 24 h (conversion determined by ^1H NMR spectroscopy = 99%). The reaction mixture was purified by reprecipitation into diethyl ether and isolated by filtration to give a block copolymer, poly(A-Pro-OMe)-*b*-poly(A-Hyp-OH): yield 0.277 g, 96%. Poly(A-Pro-OMe)-*b*-poly(A-Hyp-OH) was soluble in chloroform, acetone, methanol, and water (pH = 7) and insoluble in diethyl ether and ethyl acetate.

The copolymer composition was determined using ^1H NMR spectroscopy by a comparison of peaks associated with the two comonomers. The peak at 3.3–4.2 ppm is attributed to the methylene protons (NCH_2) of the both units and the methyl protons of A-Pro-OMe unit, whereas the peaks at 4.2–4.7 ppm correspond to the methine protons of the both units (NCHCOO) and A-Hyp-OH unit (CHOH), as shown in Figure 1a. Thus, the comonomer composition can be calculated using eq 1

$$\frac{2(x) + 5(1-x)}{2(x) + 1(1-x)} = \frac{\text{integral at 3.3–4.2 ppm}}{\text{integral at 4.2–4.7 ppm}} \quad (1)$$

where x is the fraction of the A-Hyp-OH and $1 - x$ is the fraction of A-Pro-OMe in the block copolymer.

For SEC measurements, a part of the crude product was modified by the methylation and the methylated block copolymer was directly used for SEC measurement without any purification. The methylation of the poly(A-Hyp-OH) segment in the block copolymer was conducted using trimethylsilyldiazomethane according to a method reported previously with a slight modification.^{53,54} In this way, 25 mg of the sample was dissolved in a mixture of THF/methanol (2/1 vol %), to get solubilization at room temperature, overall volume 3.0 mL. The yellow solution of trimethylsilyldiazomethane (0.50 mL, 1.00 mmol, $(\text{CH}_3)_3\text{SiCHN}_2/\text{COOH}$ group in poly(A-Hyp-OH) = 7/1 molar ratio) was added dropwise at room temperature into the polymer solution. Upon addition, bubbles appeared and the bright yellow solution became instantaneously pale yellow. After the methylation agent was added completely, the solution was stirred for 1 h more at room temperature. After removing the solvents by evaporation, the methylated samples were employed without any purification for the SEC measurements. Poly(A-Pro-OMe)-*b*-poly(A-Hyp-OMe) obtained by the methylation had an M_n (as determined by SEC) of 16 500 and a polydispersity index of 1.55, which corresponds to $M_n = 15\,700$ in the carboxylic acid form. For the UV/vis and DLS measurements, the methylated mixture was precipitated into diethyl ether. The sample was evaluated by ^1H NMR spectroscopy in CD_3OD (see Figure 1b). Poly(A-Pro-OMe)-*b*-poly(A-Hyp-OMe) obtained after the methylation was soluble in most organic solvents, such as dichloromethane, acetone, dioxane, DMF, and DMSO, and insoluble in hexane and water in the wide pH ranges (pH = 1, 7, 10).

Instrumentation. The ^1H (400 MHz) and ^{13}C NMR (100 MHz) spectra were recorded by a JEOL JNM-ECX400. The circular dichroism (CD) was measured by a JASCO J-720 spectropolarimeter. The UV–vis spectra were recorded using a JASCO V-630BIO UV–vis spectrophotometer. FT-IR spectra were obtained with a JASCO FT/IR-210 spectrometer.

The number-average molecular weight (M_n) and molecular weight distribution (M_w/M_n) were estimated by size-exclusion chromatography (SEC) using a Tosoh HPLC HLC-8220 system equipped with refractive index and ultraviolet detectors at $40\text{ }^\circ\text{C}$. The column set was as follows: four consecutive hydrophilic vinyl polymer-based gel columns [TSK-GELs (bead size, exclusion limited molecular weight): $\alpha\text{-M}$ ($13\text{ }\mu\text{m}$, $>1 \times 10^7$), $\alpha\text{-4000}$ ($10\text{ }\mu\text{m}$, 4×10^5), $\alpha\text{-3000}$ ($7\text{ }\mu\text{m}$, 9×10^4), $\alpha\text{-2500}$ ($7\text{ }\mu\text{m}$, 5×10^3), 30 cm each] and a guard column [TSK guard column α , 4.0 cm]. The system was operated at the flow rate of 1.0 mL/min using DMF containing 10 mM LiBr as the eluent. Polystyrene standards (Tosoh) ranging from 1050 to 1 090 000 were employed for calibration.

The phase separation temperatures of the aqueous solutions of the polymers (2.0 mg/mL) were measured by monitoring the transmittance of a 500 nm light beam through a quartz sample cell. The transmittance was recorded on a JASCO V-630BIO UV–vis spectrophotometer equipped with temperature controller system (JASCO EHC-716 and EHC-717). The temperature was increased at a rate of $1.0\text{ }^\circ\text{C}/\text{min}$ in heating scans between 10 and $70\text{ }^\circ\text{C}$. Dynamic light scattering (DLS) was performed at room temperature by an Otsuka Electronics DLS-7000 spectrometer with a He–Ne laser ($\lambda_0 = 632.8\text{ nm}$) at the scattering angle of 90° . Prior to the light scattering measurements, the polymer solutions were filtered using Millipore Teflon filters with a pore size of $0.2\text{ }\mu\text{m}$ into a dust-free cylindrical cuvette. Height and phase images were observed by a Multimode scanning force microscopy (SFM) operated in Tapping Mode. All measurements were conducted using Nanoscope IIIa (Veeco), and the images were acquired in ambient conditions at room temperature. The samples were prepared by spin-coating from aqueous solution onto a freshly cleaved mica surface.

Table 1. Synthesis of Block Copolymers by Polymerization of *N*-Acryloyl-4-*trans*-hydroxy-L-proline (A-Hyp-OH) Using 2,2'-Azobis(isobutyronitrile) and Poly(*N*-acryloyl-L-proline methyl ester), Poly(A-Pro-OMe), as a Macro-CTA in *N,N*-Dimethylformamide (DMF) at 60 °C for 24 h^a

run	[M]/[macro-CTA]	conv ^b (%)	M_n^c (theory)	M_n^d (NMR)	M_n^e (SEC)	M_w/M_n^e (SEC)	A-Pro-OMe/A-Hyp-OH composition	
							calcd ^f	obsd ^b
1	25	99	11 200	14 000	15 100	1.20	59:41	60:40
2	50	99	15 800	16 200	16 500	1.55	42:58	45:55
3	100	98	22 200	23 000	25 000	1.58	27:73	27:73

^a [Macro-CTA]/[AIBN] = 2, monomer concentration = 0.25 g/mL, macro-CTA (M_n = 6600, M_w/M_n = 1.27). ^b Calculated by ¹H NMR. ^c Theoretical molecular weight ($M_{n,theory}$) = (MW of A-Hyp-OMe) × [A-Hyp-OH]/[macro-CTA] × conversion + (MW of macro-CTA), A-Hyp-OMe = *N*-acryloyl-4-*trans*-hydroxy-L-proline methyl ester. ^d Evaluated by M_n value of the macro-CTA, and the composition of the block copolymer determined by ¹H NMR. ^e Methylated samples were measured by SEC using polystyrene standards in *N,N*-dimethylformamide (DMF, 0.01 M LiBr). ^f Calculated from the monomer conversion, M_n value of the macro-CTA, and the monomer composition in the feed.

Results and Discussion

Synthesis of Block Copolymers. In a previous communication, we reported that polymerization of A-Pro-OMe with benzyl dithiobenzoate in chlorobenzene at 60 °C afforded the nearly monodispersed poly(A-Pro-OMe)s with controlled molecular weights.⁴⁵ It was also demonstrated that most of the chain ends of the poly(A-Pro-OMe) were functionalized with the dithioester end groups, which could be used as a macro-CTA for further chain extension reactions.⁴⁸ Furthermore, good control of the polymerization of A-Hyp-OH was attained by RAFT polymerization with the benzyl dithiobenzoate.⁵⁰ For the controlled synthesis of dual thermo-responsive block copolymers derived from L-proline derivatives, therefore we conducted RAFT polymerization of A-Hyp-OH using the poly(A-Pro-OMe) macro-CTA having the dithiobenzoate end group, as shown in Scheme 2.

Initially, the dithiobenzoate-terminated poly(A-Pro-OMe) having a relatively low molecular weights (M_n = 6600, M_w/M_n = 1.27) was prepared by RAFT polymerization of A-Pro-OMe with benzyl dithiobenzoate. The synthesis of block copolymer was conducted by the polymerization of A-Hyp-OH using the dithiobenzoate-terminated poly(A-Pro-OMe) as a macro-CTA in DMF at 60 °C for 24 h, keeping the macro-CTA to initiator ratio at a constant value of [macro-CTA]₀/[AIBN]₀ = 2/1. The monomer to macro-CTA ratio ([A-Hyp-OH]₀/[macro-CTA]₀) was varied from 25 to 100, in order to control the comonomer content and the molecular weight. Under the conditions, the conversions determined by ¹H NMR were almost quantitative (>97%) in all cases. As shown in Table 1, the composition of each segment and molecular weights of the resulting block copolymers could be adjusted by the [A-Hyp-OH]₀/[macro-CTA]₀ ratio in the feed. In the ¹H NMR spectrum of the block copolymer measured in CD₃OD, the peaks corresponding to both components are clearly detected (Figure 1). The compositions of the copolymers determined by ¹H NMR are in reasonable agreement with the calculated values from the conversion and feed ratios of both monomers, irrespective of the comonomer ratio in the feed. Figure 2 shows the SEC chromatograms of the starting macro-CTA and growth polymers, which were obtained by the polymerization, followed by the methylation of the carboxylic acid groups. A shift in the SEC trace toward higher molecular ranges can be observed as the [A-Hyp-OH]/[macro-CTA] ratio increases. The SEC traces are unimodal with no evidence of high molecular weight species. The relatively higher molecular weight products obtained at [A-Hyp-OH]₀/[macro-CTA]₀ = 50–100 (entries 2 and 3 in Table 1) lead to broader polydispersities, compared to that of the block copolymer having lower molecular weight. This may be due to relatively high molecular weights of the resulting products with increased viscosities at the end of the polymerization. Nevertheless, the dithiobenzoate-terminated poly(A-Pro-OMe) macro-CTA can be successfully employed for

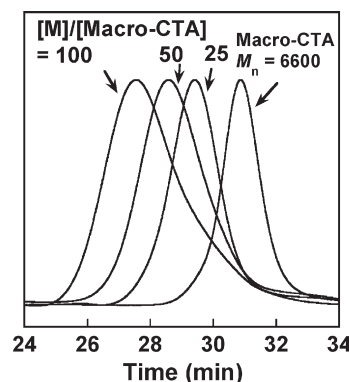


Figure 2. SEC traces of the parent poly(A-Pro-OMe) macro-CTA and the block copolymers obtained by polymerization of A-Hyp-OH using the dithiobenzoate-terminated poly(A-Pro-OMe) at different [A-Hyp-OH]/[macro-CTA] ratios, followed by the methylation. See Table 1 for detailed polymerization conditions.

the synthesis of the proline-based block copolymer with a relatively narrow polydispersity, controlled molecular weights, and predetermined composition. These results suggest a sufficient efficiency of the fragmentation from the intermediate radical to the dithiobenzoate-terminated poly(A-Pro-OMe) radical combined with an efficient reinitiation, resulting in the rapid conversion of the macro-CTA to the block copolymer under the condition used in this study.

As a comparison, we synthesized proline-based random copolymers by RAFT copolymerization of A-Pro-OMe with A-Hyp-OH, by which appropriate hydrophilic/hydrophobic balance can be achieved. The copolymerization via RAFT process was conducted with benzyl 1-pyrrolicarboxy dithioate as CTA (see Supporting Information) in DMF at 60 °C at different A-Pro-OMe:A-Hyp-OH molar ratios in the feed at ([A-Pro-OMe] + [A-Hyp-OH])/[CTA] = 100 and [CTA]/[AIBN] = 2 according to the procedure reported previously.⁵⁰ Depending on the comonomer ratio (A-Pro-OMe:A-Hyp-OH = 75:25, 50:50, 25:75) in the feed, the copolymers with number-average molecular weights between 13 500 and 15 000 and the A-Pro-OMe content between 31 and 75% were obtained quantitatively (yield = 88–94%; see Table S1, Supporting Information). In all cases, the compositions of the copolymers determined by ¹H NMR are in reasonable agreement with the calculated values from the conversion and the feed ratio of both monomers. The polydispersity indices (M_w/M_n) for all samples ranged between 1.31 and 1.39. The molecular weight distribution and the comonomer composition of the resulting random copolymers are comparable to those of block copolymers.

Block Copolymers Exhibiting Upper and Lower Critical Solution Temperatures. In this study, poly(A-Pro-OMe) was selected as a thermoresponsive segment, whereas the poly(A-Hyp-OH) was selected as a strong hydrophilic polymer as

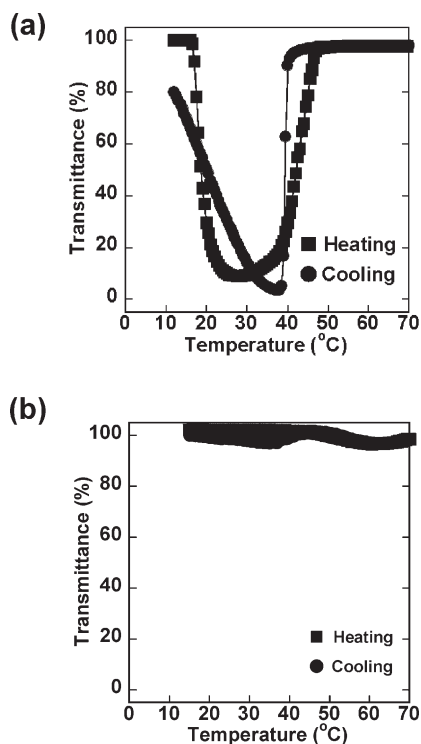


Figure 3. Temperature dependence of the transmittance at 500 nm of aqueous solutions (polymer concentration = 2.0 mg/mL, pH = 2, NaCl concentration = 0.1 M) of (a) block copolymer, poly(A-Pro-OMe)₂₇-*b*-poly(A-Hyp-OH)₇₃ ($M_n = 25\,000$, $M_w/M_n = 1.58$) and (b) random copolymer, poly(A-Pro-OMe)₃₁-*r*-poly(A-Hyp-OH)₆₉ ($M_n = 15\,000$, $M_w/M_n = 1.39$).

well as a weak polyelectrolyte. Poly(A-Pro-OMe) was soluble in most organic solvents, such as dichloromethane, chloroform, acetone, ethyl acetate, THF, 1,4-dioxane, methanol, DMF, and DMSO, while insoluble in diethyl ether and hexane. In contrast, poly(A-Hyp-OH) was soluble in water independent of pH value, methanol, ethanol, DMSO, and DMF. The nature of each component and specific interactions involving hydrogen-bonding, acid–base interactions, and oppositely charged ionic interactions should be contributed to characteristic thermosensitive properties in aqueous media.

We initially evaluated thermally induced phase separation behaviors of poly(A-Pro-OMe)₂₇-*b*-poly(A-Hyp-OH)₇₃ in an acidic water (polymer concentration = 2.0 mg/mL, pH = 2, NaCl concentration = 0.1 M), as monitored by UV (500 nm), in which the heating rate was fixed at 1.0 °C/min. As can be seen in Figure 3a, the block copolymer was soluble in water at low temperature (< 20 °C), which undergo a clear phase transition upon heating. The transmittance decreased drastically during 19–21 °C, indicating that a sharp LCST-type phase separation (T_{p1}) occurred. White turbid solution (transmittance < 20%) was kept constant between 20 and 40 °C. Further increase in the solution temperature led to the sharp increase in the transmittance during 39–45 °C, suggesting the presence of UCST-type phase separation (T_{p2}). When the transparent solution was cooled, it returned to the white turbid solution, and then the transmittance increased gradually without clear phase separation. Repeating of these heating and cooling cycles showed the same phase separation behaviors (see Figure S1, Supporting Information), suggesting the stability of the polymers under the conditions. In the absence of salt, the block copolymer also revealed a reentrant soluble–insoluble–soluble transition with increasing temperature

under the acidic condition (see Figure S2, Supporting Information). These results suggest that the proline-based block copolymer shows characteristic dual thermoresponsive properties with hysteresis, in which both LCST and UCST can be detected on heating whereas only UCST-type transition can be observed on cooling.

Thermally induced phase separation behavior of the block copolymer, poly(A-Pro-OMe)₂₇-*b*-poly(A-Hyp-OH)₇₃, was compared with the corresponding random copolymer under the same conditions. As shown in Figure 3b, the random copolymer having a similar comonomer composition (A-Hyp-OH content = 69%) was soluble in water, and clear transparent solution was observed independent of the temperature, indicating no soluble–insoluble–soluble transitions. This may be due to the fact that relatively homogeneous distribution of A-Hyp-OH component in the random copolymer leads to the formation of only short poly(A-Pro-OMe) segments having no thermoresponsive property, resulting in the increase of the water solubility.

Since A-Hyp-OH has a carboxylic acid and a hydroxyl group in the monomer unit, poly(A-Hyp-OH) can be recognized as a weak polyelectrolyte, in which the degree of ionization is governed by the pH and ionic strength of the aqueous solution. Hence, the thermoresponsive properties of the block copolymers having poly(A-Hyp-OH) segment are expected to be affected by the pH value, even if poly(A-Hyp-OH) is soluble in water in all pH ranges (see Figures S3 and S4, Supporting Information). Additionally, thermally induced phase separation behavior of poly(A-Pro-OMe) was slightly affected by pH values (see Figures S5 and S6, Supporting Information). In order to clarify this point, the thermally induced phase separation behaviors of poly(A-Pro-OMe)₂₇-*b*-poly(A-Hyp-OH)₇₃ was investigated in water at different pH values. As shown in Figure 4a, the block copolymer exhibits a clear soluble–insoluble phase transition upon heating at pH = 1, and then the transmittance increases gradually without clear phase separation. On cooling, a clear soluble–insoluble transition is detected at 56–58 °C, which is apparently higher than that at pH = 2 (Figure 4b). At pH = 3, no detectable transition was seen on heating and cooling, indicating that the protonation of the carboxylic acid in A-Hyp-OH unit is required to account for the unique phase transition behavior. These results suggest that the pH value in aqueous solution affects dual thermoresponsive property, and characteristic soluble–insoluble–soluble transition of the block copolymer can be observed only on a suitable pH range. We conducted ¹H NMR measurements of representative polymers in D₂O and acidic D₂O containing a small amounts of DCl (pH = 2) at elevated temperatures. As can be seen in Figures S7–S14 (Supporting Information), no detectable peak corresponding to unfavorable degradation was observed in those samples treated under the conditions. The stabilities of the block copolymer and homopolymers were also confirmed by the repeating of the heating and cooling cycles (Figures S1, S4, and S6, Supporting Information).

Similar pH-dependent changes in the phase transitions were observed in poly(*N*-vinylacetamide-*co*-acrylic acid)s,³³ in which similar soluble–insoluble–soluble transition was detected below pH ~ 2.2, whereas the phase transition behavior disappeared above pH 3. They demonstrated that hydrogen bonding between the amide group in the vinylacetamide unit and the carboxylic acid group in the acrylic acid unit is a key factor in determining the phase transition behavior. In addition to the hydrogen bonding between the amide group in A-Pro-OMe unit and the carboxylic acid group in A-Hyp-OH unit, in our system, the existence of the

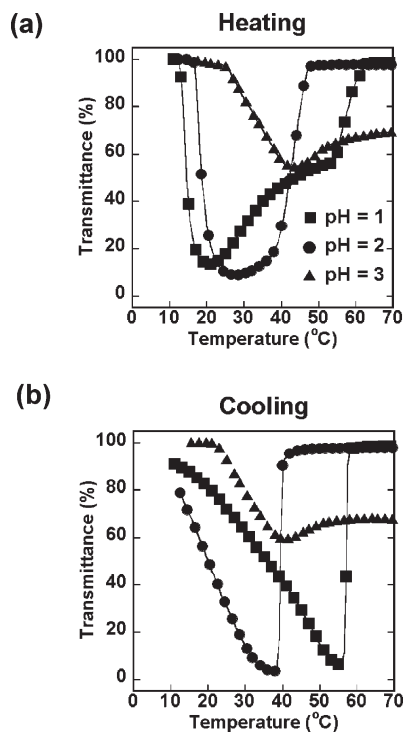


Figure 4. Temperature dependence of the transmittance at 500 nm of aqueous solutions (polymer concentration = 2.0 mg/mL, NaCl concentration = 0.1 M) of block copolymer, poly(A-Pro-OMe)₂₇-b-poly(A-Hyp-OH)₇₃ (M_n = 25 000, M_w/M_n = 1.58) at different pH values: pH = 1 (squares), 2 (circles), and 3 (triangles). (a) Heating and (b) cooling cycles.

hydroxyl group in A-Hyp-OH unit should be contributed to the formation of the hydrogen bonding and high water solubility. We previously reported that similar proline-based block copolymers comprising of A-Pro-OMe and *N*-acryloyl-L-proline, which has only a carboxylic acid moiety in the monomer unit, exhibited characteristic pH- and thermoresponsive properties.⁴⁹ However, the block copolymer showed only LCST-type soluble–insoluble transition behavior, providing the evidence that the hydroxyl group in poly(A-Hyp-OH) segment play a crucial role in the unique soluble–insoluble–soluble phase transitions.

Figure 5 shows the dependence of the solution turbidity of the block copolymers having different A-Pro-OMe contents, ranging from 27 to 45 mol %, on the temperature. As expected, the mole fraction of A-Pro-OMe was found to affect the temperature of the phase separation. In all cases, a clear LCST-type soluble–insoluble phase transition is detected upon heating, and the transition temperature is practically independent of A-Pro-OMe content (around 15–22 °C). In contrast, the UCST-type insoluble–soluble phase transition observed at low A-Pro-OMe content (27 mol %) disappears with increasing A-Pro-OMe content (Figure 5a–c). On cooling, the increase in the soluble–insoluble transition temperature is seen with increasing A-Pro-OMe content (Figure 5d–f). These results suggest that the block copolymer having suitable comonomer composition (A-Pro-OMe/A-Hyp-OH = 27/73) shows characteristic soluble–insoluble–soluble transitions, while the introduction of more A-Pro-OMe segment results in the loss of dual temperature-responsive property.

Thermally induced phase separation behavior of the random copolymers having different comonomer compositions (A-Pro-OMe/A-Hyp-OH = 31/69, 53/47, 75/25) was also investigated as a comparison (see Figure S15, Supporting

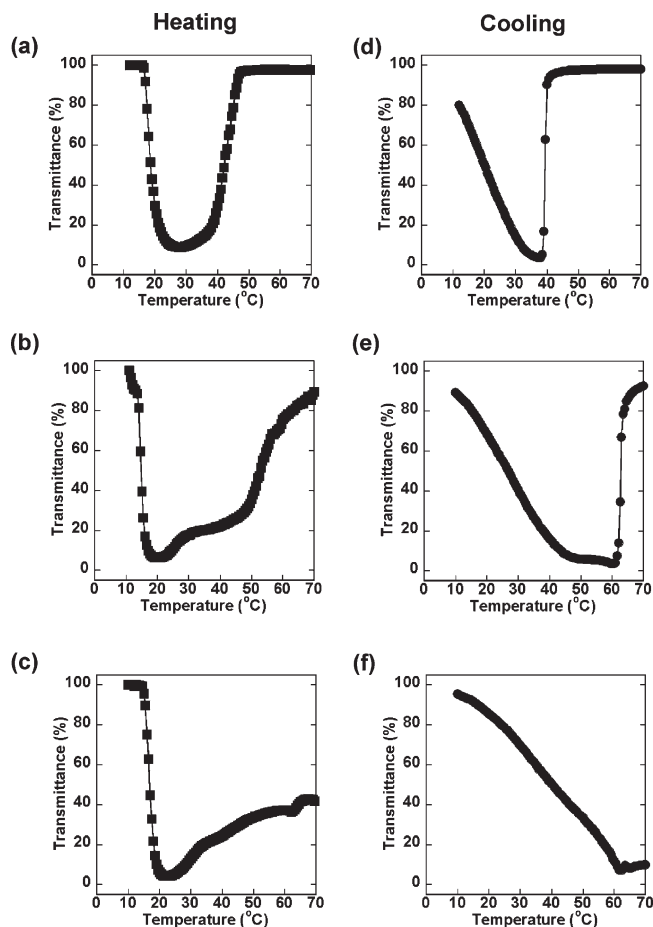


Figure 5. Temperature dependence of the transmittance at 500 nm of aqueous solutions (polymer concentration = 2.0 mg/mL, pH = 2, NaCl concentration = 0.1 M) of the block copolymers, poly(A-Pro-OMe)_{*m*}-b-poly(A-Hyp-OH)_{*n*}, having different compositions; *m*:*n* = 27:73 (a, d), 37:63 (b, e), and 45:55 (c, f). (a–c) Heating and (d–f) cooling.

Information). The random copolymers having relatively high A-Pro-OMe contents (A-Pro-OMe = 53 and 75 mol %) exhibited the LCST-type soluble–insoluble transition around 15 °C on heating, similar to the homopolymer poly(A-Pro-OMe). However, no UCST-type insoluble–soluble phase transition was detected on heating, and the transmittance increased gradually on cooling without no detectable transition.

Solution Property of Block Copolymers. Temperature-responsive solution properties of poly(A-Pro-OMe)₂₇-b-poly(A-Hyp-OH)₇₃ having both LCST and UCST type transitions were characterized using dynamic light scattering (DLS) in the acidic water (pH = 2). As shown in Figure 6a, the block copolymer shows a monomodal hydrodynamic diameter distribution in the solvent at 15 °C. The relatively narrow hydrodynamic diameter distribution most probably indicates a spherical morphology of the micelles consisting of a relatively hydrophobic core of poly(A-Pro-OMe) and a hydrophilic shell of poly(A-Hyp-OH). Note that the formation of the hydrogen bonds between the amide moiety in the both proline-based units and the carboxylic acid moiety in A-Hyp-OH may protect A-Pro-OMe groups from the exposure to water, even if poly(A-Pro-OMe) exhibits the transition temperature at around 20 °C. Figure 7a shows temperature dependence of hydrodynamic diameter (D_h) and transmittance of aqueous solution (pH = 2, concentration = 2 mg/mL) of poly(A-Pro-OMe)₂₇-b-poly(A-Hyp-OH)₇₃. A remarkable

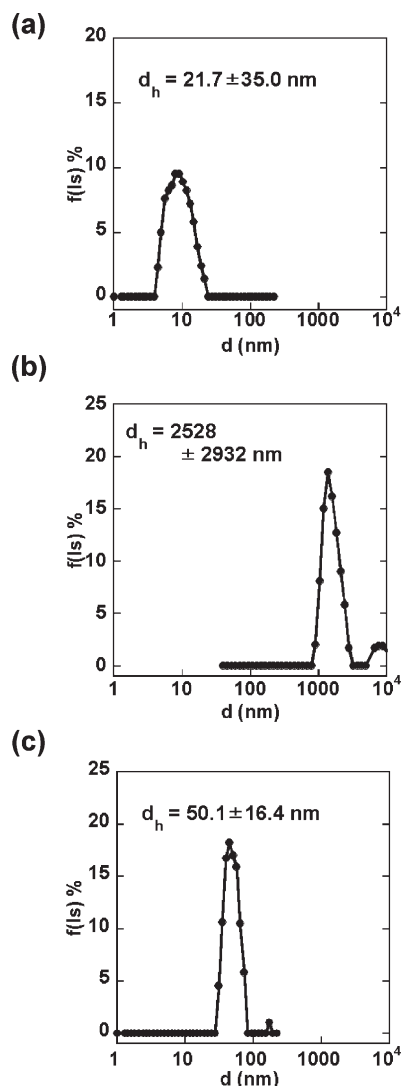


Figure 6. Hydrodynamic diameter distributions, $f(D_h)$, of the micelles obtained from poly(A-Pro-OMe)₂₇-*b*-poly(A-Hyp-OH)₇₃ in an acidic water (polymer concentration = 2 mg/mL, pH = 2, NaCl concentration = 0.1 M) at (a) 15, (b) 30, and (c) 60 °C.

increase in the diameter is observed with increasing the solution temperature; from $D_h = 22$ nm at 15 °C into about 2500 nm at 30 °C (Figure 6b), which corresponds to LCST-type soluble–insoluble transition. Further increase in the solution temperature leads to the decrease in the size; $D_h = 50$ nm at 60 °C (Figure 6c), which corresponds to UCST-type insoluble–soluble transition. Hence, both LCST and UCST behaviors were confirmed by DLS measurements.

Scanning force microscopy (SFM) was employed to visualize the assembled structure of the block copolymer, poly(A-Pro-OMe)₂₇-*b*-poly(A-Hyp-OH)₇₃. The samples were prepared by spin-coating from the aqueous solution (2.0 mg/mL, pH = 2) onto a freshly cleaved mica surface as a substrate. As shown in Figure 8a,c, spherical particles of about 10–100 nm in the diameter and 2–4 nm in height are occasionally observed clearly in the height image. The same shape and distribution are seen in the phase image (Figure 8b,d). In contrast, no assembled structure was detected on SFM measurement of a random copolymer having similar comonomer composition, poly(A-Pro-OMe)₃₁-*r*-poly(A-Hyp-OH)₆₉ prepared under the same conditions (Figure S17, see Supporting Information). These results can provide further evidence toward the presence of micelles in an acidic aqueous solution of the block copolymer at room temperature.

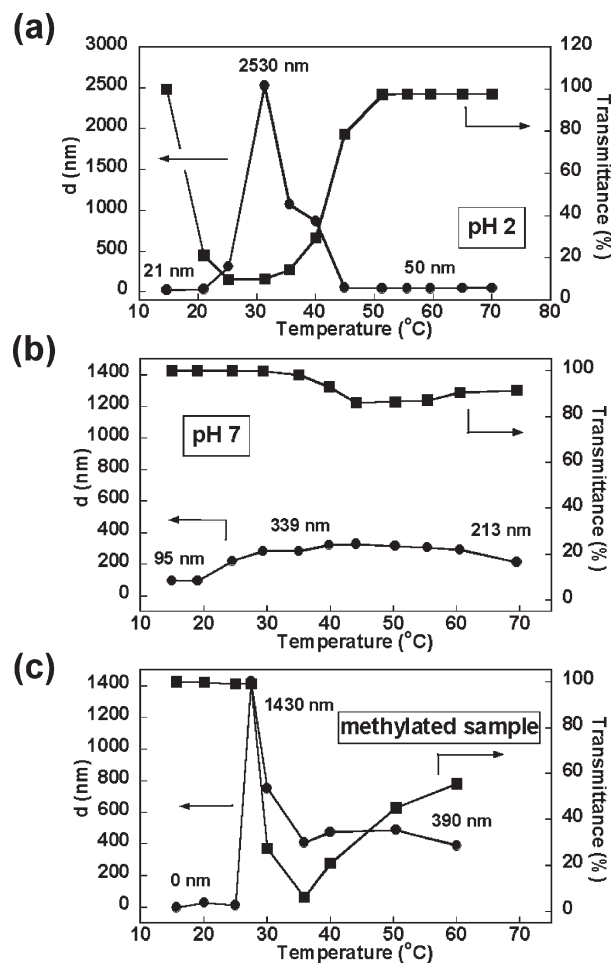


Figure 7. Temperature dependence of hydrodynamic diameter (D_h) and transmittance of aqueous solution (concentration = 2 mg/mL, NaCl concentration = 0.1 M) of poly(A-Pro-OMe)₂₇-*b*-poly(A-Hyp-OH)₇₃ at (a) pH = 2 and (b) pH = 7 and poly(A-Pro-OMe)₂₇-*b*-poly(A-Hyp-OMe)₇₃ at (c) pH = 7.

Figure 9 represents postulated mechanism of the soluble–insoluble–soluble transition observed in the acidic aqueous solution of the block copolymers, poly(A-Pro-OMe)-*b*-poly(A-Hyp-OH). Below T_{p1} , a small part of the A-Pro-OMe amide and ester groups form hydrogen bonds with the carboxyl and hydroxyl groups in A-Hyp-OH unit to afford insoluble complex, which corresponds to the hydrogen-bonded A-Pro-OMe core. Remaining A-Pro-OMe and A-Hyp-OH units in the block copolymer act as water-soluble shell to form micelle in acidic water. With increasing solution temperature, the stability of hydration around the amide groups decreases. Around the first transition temperature T_{p1} , the cooperative dehydration of the A-Pro-OMe amide groups occurs, which leads to simultaneous formations of the intra- and interchain hydrogen bonds between the carboxyl and hydroxyl groups in A-Hyp-OH unit with the amide and ester groups in A-Pro-OMe to afford insoluble aggregates. Hence, the first transition temperature T_{p1} is due to the complexation of A-Pro-OMe and A-Hyp-OH units via hydrogen bonding, which corresponds to LCST of poly(A-Pro-OMe) segment. With further increase in solution temperature, the intra- and interchain hydrogen bonding cooperatively dissociates at T_{p2} because of the activated motion of the copolymer chains. Above the second transition temperature T_{p2} , the dehydrated A-Pro-OMe core-micelle is formed with the water-soluble poly(A-Hyp-OH) shell.

The increase in T_{p2} with decreasing A-Hyp-OH content (observed in Figure 5) is attributed to the hydrogen bonding dissociation between A-Hyp-OH and A-Pro-OMe units. The carboxyl and hydroxyl groups in A-Hyp-OH unit can be

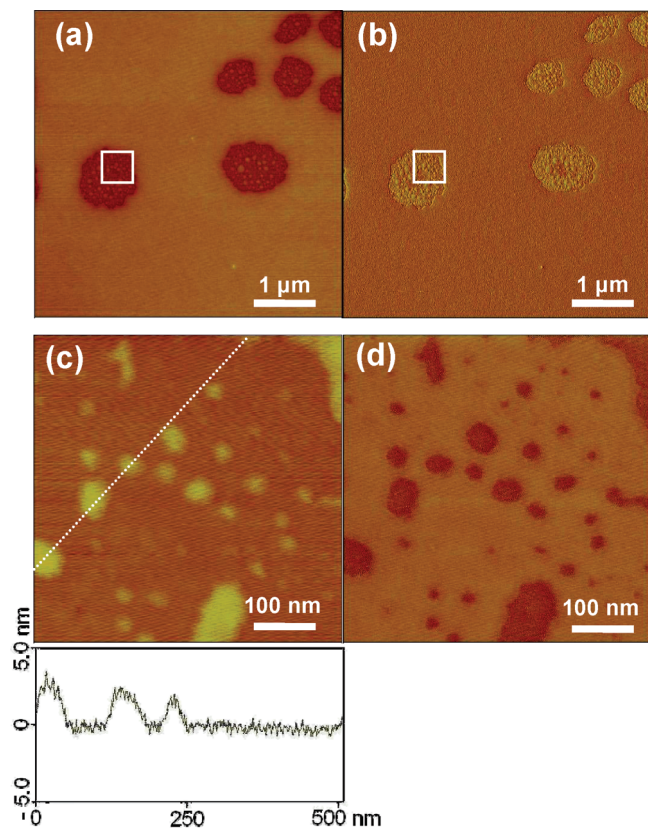


Figure 8. SFM images of poly(A-Pro-OMe)₂₇-*b*-poly(A-Hyp-OH)₇₃. The sample was prepared by spin-coating from a dilute aqueous solution (2.0 mg/mL, pH = 2) onto freshly cleaved mica. Height images (a: z -range = 50 nm; c: z -range = 20 nm), (b, d) phase images (z -range = 60°), and (c, d) higher magnification images taken from the area inside the box in (a and b). Under the magnification height image (c), we show the cross section at the position indicated by the dotted line.

acted as a proton donor. More hydrogen bonding occurs when the contents of both monomers in the copolymer become comparable. Hence, the second transition temperature T_{p2} is observed to increase with decreasing A-Hyp-OH content in the range of 55–73%. In contrast, the first transition temperature T_{p1} is the almost same under acidic conditions, regardless of the comonomer composition, as shown in Figure 5. The phenomenon may be due to the fact that a small part of the hydrogen-bonded complexation of A-Hyp-OH and A-Pro-OMe units is located predominantly in the core below T_{p1} , and the assembled structures disappear after the hydration of the A-Pro-OMe amide groups to afford insoluble aggregates.

The solution properties of the dual thermoresponsive block copolymer, poly(A-Pro-OMe)₂₇-*b*-poly(A-Hyp-OH)₇₃, was also investigated at pH = 7. As can be seen in Figure 7b, a clear transparent solution was observed independent of the temperature (the transmittance > 85%). Under the conditions, the average hydrodynamic diameter (D_h = 95 nm) observed at 15 °C increased slightly with increasing the temperature, and the maximum diameter was detected at 40 °C (D_h = 339 nm). These results suggest that higher degree of the ionization of poly(A-Hyp-OH) segment leads to the increase in the micelle sizes of poly(A-Pro-OMe)₂₇-*b*-poly(A-Hyp-OH)₇₃ at low temperature, while no turbid solution is detected upon the heating process.

At pH = 7, no detectable soluble–insoluble–soluble transition of poly(A-Pro-OMe)-*b*-poly(A-Hyp-OH) was observed (Figure 7b). This may be due to the weakening of the hydrogen bonding between the A-Hyp-OH and A-Pro-OMe because of a partial dissociation of the carboxylic acid group in A-Hyp-OH unit in this pH range. Only undissociated carboxylic acids are known to be capable of participation in hydrogen bonding because charged groups in polyelectrolyte are surrounded by small, oppositely charged counterions in aqueous solutions. At low temperature, the undissociated carboxylic acid and hydroxyl group in A-Hyp-OH unit can form hydrogen bonding with the A-Pro-OMe unit in the core of the micelle. Above LCST of the thermosensitive poly(A-Pro-OMe) segment, the dehydrated poly(A-Pro-OMe) segment is acting as the core, and poly(A-Hyp-OH) corresponds to a water-soluble shell.

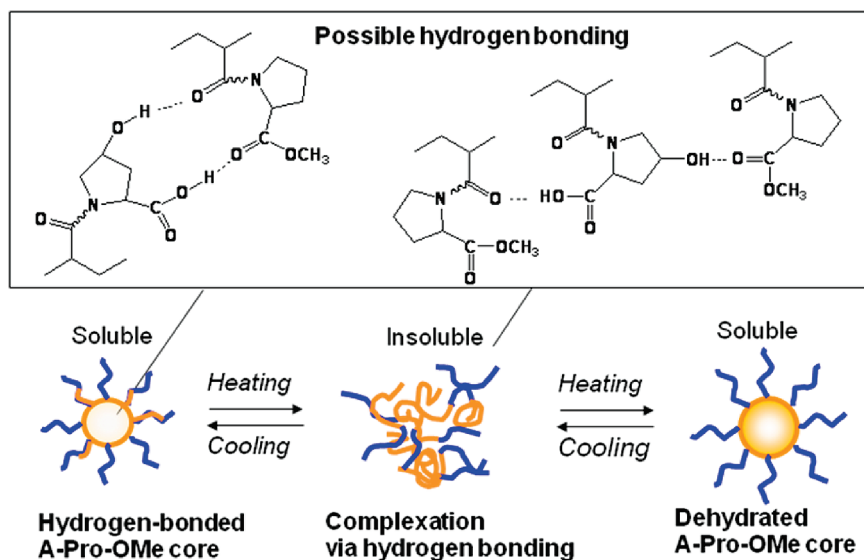


Figure 9. Postulated mechanism of the soluble–insoluble–soluble transition of the block copolymer, poly(A-Pro-OMe)-*b*-poly(A-Hyp-OH), via self-assembly and hydrogen bonding. The blue and orange blocks correspond to water-soluble poly(A-Hyp-OH) segment and thermoresponsive poly(A-Pro-OMe) segment, respectively.

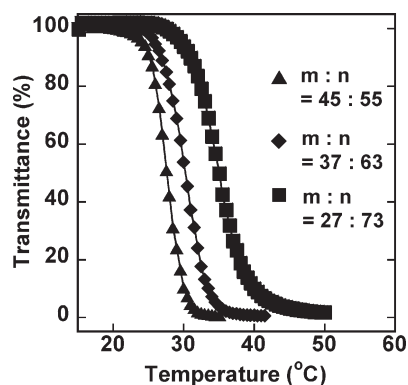


Figure 10. Temperature dependence of the transmittance at 500 nm of aqueous solutions (polymer concentration = 2.0 mg/mL, pH = 2) of poly(A-Pro-OMe)_m-*b*-poly(A-Hyp-OMe)_n.

Block Copolymers with Blocks Having Two Lower Critical Solution Temperatures. We previously reported that the methylation reaction of the carboxylic acid groups in poly(A-Hyp-OH) led to thermoresponsive poly(A-Hyp-OMe) showing LCST type soluble–insoluble phase transition, and the transition temperature (49.5 °C) was higher than that of poly(A-Pro-OMe) (17.5 °C).⁵⁰ Furthermore, it was demonstrated that the transition temperature of the random copolymers comprising of A-Pro-OMe and A-Hyp-OMe could be manipulated by the monomer composition. In this study, the block copolymers with blocks having different LCSTs; poly(A-Pro-OMe) and poly(A-Hyp-OMe) were synthesized by the methylation reaction of the carboxylic acid groups in poly(A-Pro-OMe)-*b*-poly(A-Hyp-OH), which was obtained by RAFT polymerization. Figure 10 shows the dependence of the solution turbidity of the block copolymers having different A-Hyp-OMe contents on the temperature. The transmittance decreased sharply in all aqueous solutions at specific temperatures on heating, indicative of one step LCST-type phase transition. No detectable two-step phase separations were observed in this system. The increase in the mole fraction of A-Hyp-OMe leads to the increase in the temperature of the phase separation in aqueous solution, and the transition temperatures are intermediates between the poly(A-Pro-OMe) and poly(A-Hyp-OMe). The phase separation occurred with a similar sensitivity in all cases, irrespective of the comonomer ratios. The tendencies were almost the same to those of corresponding random copolymers having similar molecular weights and compositions (Figure S16, see Supporting Information). In both copolymers, one step LCST-type phase transition was observed, and the LCST increased with increasing A-Hyp-OMe content. The transition curves of the block copolymers having similar comonomer contents and molecular weights are slightly slower than those of the random copolymers. The slight difference in the transition behaviors between the random and block copolymers observed in this study is considered to be attributed to the micelle formation of the block copolymers.

Figure 7c compares the thermally induced phase separation behavior and solution property of poly(A-Pro-OMe)₂₇--*b*-poly(A-Hyp-OMe)₇₃, which was prepared by the methylation of the carboxylic acid moiety of poly(A-Hyp-OH) segment. The solution property was investigated by DLS studies to confirm the formation of the assembled structures. At 15–25 °C, no assembled structure was detected, suggesting that both poly(A-Pro-OMe) and poly(A-Hyp-OMe) segments are soluble completely and the block copolymer behaved as an unimolecular. The drastic increase in the size

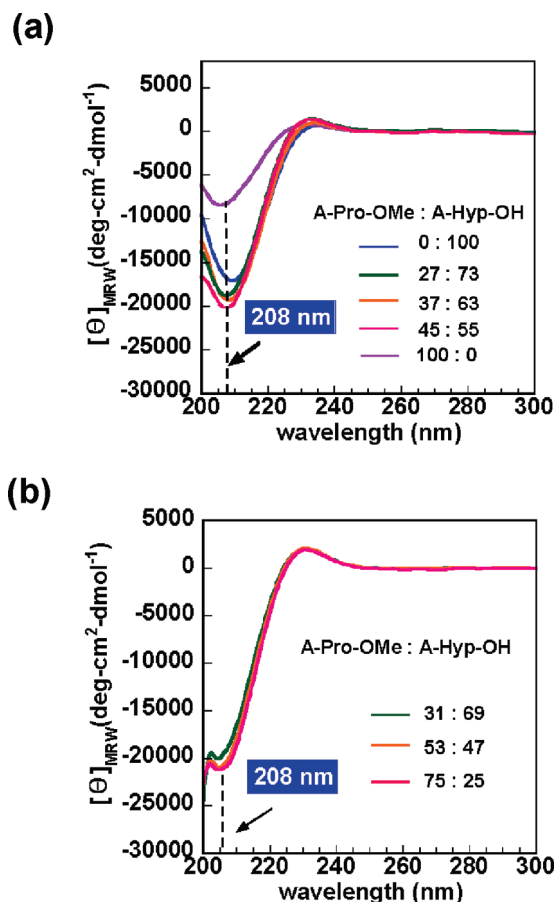


Figure 11. CD spectra of (*c* = 0.03 mg/mL) of (a) the block copolymers having different compositions, poly(A-Pro-OMe)_m-*b*-poly(A-Hyp-OH)_n, and (b) the corresponding random copolymers, poly(A-Pro-OMe)_m-*co*-A-Hyp-OH_n in a neutral water (pH = 7, NaCl concentration = 0.1 M).

was observed at 25–30 °C, which may be due to the aggregation. The transition temperature determined by DLS is comparable to the LCST-type soluble–insoluble transition observed at 27–30 °C. Then, the size decreased gradually with increasing the temperature.

Chiroptical Property of Block Copolymers. In terms of chirality, poly(A-Pro-OMe)-*b*-poly(A-Hyp-OH) prepared in this study can be classified into chiral–chiral (L–L) type block copolymer. The chiroptical behavior of the block copolymer, which is related to the conformation of polymers in solution, was investigated by CD measurement. Figure 11 depicts the CD spectra of the block copolymers having different compositions, poly(A-Pro-OMe)_m-*b*-poly(A-Hyp-OH)_n, and corresponding random copolymers in a neutral water (pH = 7, NaCl concentration = 0.1 M, polymer concentration = 0.03 mg/mL). Under the conditions, all block and random copolymers were soluble in the neutral water at room temperature, independent of the composition. The block copolymers show a strong negative signal at 208 nm, which is very probably attributed to the $n \rightarrow \pi^*$ transitions of the carboxyl chromophore.⁵⁵ The peak intensities of the negative peaks of the block copolymers (−18 000 to −22 000 deg cm² dmol^{−1}) are comparable to that of poly(A-Hyp-OH), which is apparently higher than that of poly(A-Pro-OMe). As can be seen in Figure 11a,b, no detectable difference in the peak intensities between block and random copolymers is seen, suggesting no significant contribution of the block structures on the specific conformation in the basic water. In both cases, a positive signal is

visible at around 230 nm, which is attributed to the $\pi_1 \rightarrow \pi^*$ transition of the amide chromophore.⁵⁵

Conclusion

Novel dual thermoresponsive block copolymer, poly(*N*-acryloyl-L-proline methyl ester)-*b*-poly(*N*-acryloyl-4-*trans*-hydroxy-L-proline), poly(A-Pro-OMe)-*b*-poly(A-Hyp-OH), was synthesized by RAFT polymerization of two proline-based monomers. The block copolymer having suitable comonomer composition (A-Pro-OMe/A-Hyp-OH = 27/73) exhibited the reentrant soluble–insoluble–soluble transition with hysteresis in acidic water, in which both LCST- and UCST-type transitions were detected on heating, whereas only indistinct UCST-type transition was observed on cooling. By applying the transformation of the carboxylic acid to the methyl ester group (from A-Hyp-OH to A-Hyp-OMe), we obtained block copolymers with blocks having different LCSTs, poly(A-Pro-OMe)-*b*-poly(A-Hyp-OMe), which showed one-step phase separation. This work presents the first report on controlled synthesis of proline-based block copolymer showing LCST and UCST, which can be easily transformed into another type of dual thermoresponsive block copolymer having two different LCSTs.

Acknowledgment. This work has been supported by a Grant-in-Aid for Scientific Research from the Ministry of Education, Culture, Sports, Science, and Technology, Japan (19550118).

Supporting Information Available: Figures showing temperature dependence of the transmittance of the block copolymers and homopolymers under various conditions (three repeated cycles, with and without NaCl, different pH values), random copolymers having different compositions, methylated random copolymers, ¹H NMR spectra of representative block copolymer and homopolymers in D₂O and acidic D₂O at elevated temperatures, SFM images of a random copolymer, and table showing summary of random copolymerization of A-Pro-OMe and A-Hyp-OH with experimental procedure. This material is available free of charge via the Internet at <http://pubs.acs.org>.

References and Notes

- Osada, Y.; Gong, J.-P. *Adv. Mater. (Weinheim, Ger.)* **1998**, *10* (11), 827–837.
- Petka, W. A.; Hardin, J. L.; McGrath, K. P.; Wirtz, D.; Tirrell, D. A. *Science (Washington, DC, U.S.)* **1998**, *281* (5375), 389–392.
- Mori, H.; Müller, A. H. E.; Klee, J. E. *J. Am. Chem. Soc.* **2003**, *125* (13), 3712–3713.
- Nath, N.; Chilkoti, A. *Adv. Mater. (Weinheim, Ger.)* **2002**, *14* (17), 1243–1247.
- Jeong, B.; Gutowska, A. *Trends Biotechnol.* **2002**, *20* (7), 305–311.
- Hoffman, A. S.; Stayton, P. S.; Bulmus, V.; Chen, G.; Chen, J.; Cheung, C.; Chilkoti, A.; Ding, Z.; Dong, L.; Fong, R.; Lackey, C. A.; Long, C. J.; Miura, M.; Morris, J. E.; Murthy, N.; Nabeshima, Y.; Park, T. G.; Press, O. W.; Shimoboji, T.; Shoemaker, S.; Yang, H. J.; Monji, N.; Nowinski, R. C.; Cole, C. A.; Priest, J. H.; Milton Harris, J.; Nakamae, K.; Nishino, T.; Miyata, T. *J. Biomed. Mater. Res.* **2000**, *52* (4), 577–586.
- Gil, E. S.; Hudson, S. M. *Prog. Polym. Sci.* **2004**, *29*, 1173–1222.
- Rodríguez-Hernández, J.; Chécot, F.; Gnanou, Y.; Lecommandoux, S. *Prog. Polym. Sci.* **2005**, *30* (7), 691–724.
- Motokawa, R.; Morishita, K.; Koizumi, S.; Nakahira, T.; Annaka, M. *Macromolecules* **2005**, *38*, 5748–5760.
- Arotçaréna, Michel; Bettina Heise, S.; shaya, S. I.; Laschewsky, A. *J. Am. Chem. Soc.* **2002**, *3787*–3793.
- Schilli, C. M.; Zhang, M.; Rizzardo, E.; Thang, S. H.; Chong, Y. K.; Edwards, K.; Karlsson, G.; Müller, A. H. E. *Macromolecules* **2004**, *37*, 7861–7866.
- Chen, G.; Hoffman, A. S. *Nature* **1995**, *373* (6509), 49–52.
- Dimitrov, I.; Trzebicka, B.; Müller, A. H. E.; Dworak, A.; Tsvetanov, C. B. *Prog. Polym. Sci.* **2007**, *32*, 1275–1343.
- Rzaev, Z. M. O.; Dincer, S.; Piskin, E. *Prog. Polym. Sci.* **2007**, *32*, 534–595.
- Liu, S.; Billingham, N. C.; Armes, S. P. *Angew. Chem., Int. Ed.* **2001**, *40* (12), 2328–2331.
- Nuopponen, M.; Tenhu, H. *Langmuir* **2007**, *23*, 5352–5357.
- Fournier, D.; Hoogenboom, R.; Thijs, H. M. L.; Paulus, R. M.; Schubert, U. S. *Macromolecules* **2007**, *40*, 915–920.
- Determan, M. D.; Cox, J. P.; Seifert, S.; Thiagarajan, P.; Mallapragada, S. K. *Polymer* **2005**, *46*, 6933–6946.
- Meyer, M.; Schlaad, H. *Macromolecules* **2006**, *39*, 3967–3970.
- Smith, A. E.; Xu, X.; Abell, T. U.; Kirkland, S. E.; Hensarling, R. M.; McCormick, C. L. *Macromolecules* **2009**, *42*, 2958–2964.
- Klaikherd, A.; Nagamani, C.; Thayumanavan, S. *J. Am. Chem. Soc.* **2009**, *131*, 4830–4838.
- Mertoglu, M.; Garnier, S.; Laschewsky, A.; Skrabania, K.; Storsberg, J. *Polymer* **2005**, *46*, 7726–7740.
- Sugihara, S.; Kanaoka, S.; Aoshima, S. *Macromolecules* **2005**, *38*, 1919–1927.
- Dimitrov, P.; Rangelov, S.; Dworak, A.; Tsvetanov, C. B. *Macromolecules* **2004**, *37*, 1000–1008.
- Hua, F.; Jiang, X.; Zhao, B. *Macromolecules* **2006**, *39*, 3476–3479.
- Li, C.; Buurma, N. J.; Haq, I.; Turner, C.; Armes, S. P.; Castelletto, V.; Hamley, I. W.; Lewis, A. L. *Langmuir* **2005**, *21*, 11026–11033.
- Huglin, M. B.; Radwan, M. A. *Polym. Int.* **1991**, *26*, 97–104.
- Buscall, R.; Corner, T. *Eur. Polym. J.* **1982**, *18*, 967–974.
- Virtanen, J.; Arotçaréna, M.; Heise, B.; Ishaya, S.; Laschewsky, A.; Tenhu, H. *Langmuir* **2002**, *18*, 5360–5365.
- Weaver, J. V. M.; Armes, S. P.; Bütün, V. *Chem. Commun.* **2002**, 2122–2123.
- Maeda, Y.; Mochiduki, H.; Ikeda, I. *Macromol. Rapid Commun.* **2004**, *25*, 1330–1334.
- Bokias, G.; Staikos, G.; Iliopoulos, I. *Polymer* **2000**, *41*, 7399–7405.
- Mori, T.; Nakashima, M.; Fukuda, Y.; Minagawa, K.; Tanaka, M.; Maeda, Y. *Langmuir* **2006**, *22*, 4336–4342.
- Moad, G.; Rizzardo, E.; Thang, S. H. *Aust. J. Chem.* **2005**, *58* (6), 379–410.
- McCormick, C. L.; Lowe, A. B. *Acc. Chem. Res.* **2004**, *37*, 312–325.
- Barner-Kowollik, C.; Davis, T. P.; Heuts, J. P. A.; Stenzel, M. H.; Vana, P.; Whittaker, M. *J. Polym. Sci., Part A: Polym. Chem.* **2003**, *41* (3), 365–375.
- Perrier, S.; Takolpuckdee, P. *J. Polym. Sci., Part A: Polym. Chem.* **2005**, *43* (22), 5347–5393.
- Favier, A.; Charreyre, M.-T. *Macromol. Rapid Commun.* **2006**, *27*, 653–692.
- Moad, G.; Rizzardo, E.; Thang, S. *Aust. J. Chem.* **2006**, *59* (10), 669–692.
- Lowe, A. B.; McCormick, C. L. *Prog. Polym. Sci.* **2007**, *32*, 283–351.
- ten Cate, M. G. J.; Rettig, H.; Bernhardt, K.; Börner, H. G. *Macromolecules* **2005**, *38*, 10643–10649.
- Lokitz, B. S.; Convertine, A. J.; Ezell, R. G.; Heidenreich, A.; Li, Y.; McCormick, C. L. *Macromolecules* **2006**, *39*, 8594–8602.
- Lokitz, B. S.; Stempka, J. E.; York, A. W.; Li, Y.; Goel, H. K.; Bishop, G. R.; McCormick, C. L. *Aust. J. Chem.* **2006**, *59*, 749–754.
- Boyer, C.; Bulmus, V.; Liu, J.; Davis, T. P.; Stenzel, M. H.; Barner-Kowollik, C. *J. Am. Chem. Soc.* **2007**, *129*, 7145–7154.
- Mori, H.; Iwaya, H.; Nagai, A.; Endo, T. *Chem. Commun. (Cambridge, U.K.)* **2005**, 4872–4874.
- Mori, H.; Iwaya, H.; Endo, T. *Macromol. Chem. Phys.* **2007**, *208*, 1908–1918.
- Skey, J.; O'Reilly, R. K. *J. Polym. Sci., Part A: Polym. Chem.* **2008**, *46*, 3690–3702.
- Mori, H.; Iwaya, H.; Endo, T. *React. Funct. Polym.* **2007**, *67*, 916–927.
- Mori, H.; Kato, I.; Endo, T. *Macromolecules* **2009**, *42*, 4985–4992.
- Mori, H.; Kato, I.; Matsuyama, M.; Endo, T. *Macromolecules* **2008**, *41*, 5604–5615.
- Sanda, F.; Kamatani, J.; Handa, H.; Endo, T. *Macromolecules* **1999**, *32*, 2490–2494.
- Chong, Y. K.; Krstina, J.; Le, T. P. T.; Moad, G.; Postma, A.; Rizzardo, E.; Thang, S. H. *Macromolecules* **2003**, *36*, 2256–2272.
- Couvreux, L.; Lefay, C.; Belleney, J.; Charleux, B.; Guerret, O.; Magnet, S. *Macromolecules* **2003**, *36*, 8260–8267.
- Mori, H.; Matsuyama, M.; Sutoh, K.; Endo, T. *Macromolecules* **2006**, *39*, 4351–4360.
- Morcellet-Sauvage, J.; Morcellet, M.; Loucheux, C. *Macromolecules* **1983**, *16*, 1564–1570.